

Electronic and optical properties of ternary alloys $\text{Zn}_x\text{Cd}_{1-x}\text{S}$, $\text{Zn}_x\text{Cd}_{1-x}\text{Se}$, $\text{ZnS}_x\text{Se}_{1-x}$, $\text{Mg}_x\text{Zn}_{1-x}\text{Se}$

K. BENCHIKH*, H. ABID, M. BENCHEHIMA

Applied Materials Laboratory, Djillali Liabes University, Sidi-Bel-Abbes 22000, Algeria

The empirical pseudopotential method (EPM) within the virtual crystal approximation (VCA) is used to calculate the electronic and optical properties of ternary alloys $\text{Zn}_x\text{Cd}_{1-x}\text{S}$, $\text{Zn}_x\text{Cd}_{1-x}\text{Se}$, $\text{ZnS}_x\text{Se}_{1-x}$ and $\text{Mg}_x\text{Zn}_{1-x}\text{Se}$. The alloy band structures and energy gaps are calculated using VCA which incorporates the compositional disorder as an effective potential. The calculated band structures for the $\text{Zn}_x\text{Cd}_{1-x}\text{S}$, $\text{Zn}_x\text{Cd}_{1-x}\text{Se}$ and $\text{ZnS}_x\text{Se}_{1-x}$ alloys show a direct band gap in the whole range of the concentration except for the $\text{Mg}_x\text{Zn}_{1-x}\text{Se}$ alloy which presents a crossover from the direct gap to the indirect one. Also the dependence of the refractive index on the concentration is calculated for each ternary alloy. This parameter is found to depend nonlinearly on the alloy concentration. A detailed comparison of our results with experimental data and works of other authors has led to a good agreement.

Keywords: *electronic properties; pseudopotential; alloys; zinc-blende; VCA*

© Wrocław University of Science and Technology.

1. Introduction

A particular attention has been devoted in the literature to the wide-gap semiconductor alloys for applications in the fields of optical devices technology [1, 2]. Several authors have investigated different kinds of materials in order to search for the desired parameters, such as band-gap, lattice constant, dielectric constant and carrier mobility [3–6]. In recent years, the wide gap II-VI semiconductor compounds have attracted much interest for their applications in optoelectronic devices.

Various methods for fabricating chemical compound semiconductor nanostructures have been used. For II-VI compounds, especially of ZnSe, ZnS and their alloys, the epitaxial layers were grown on substrates by the metalorganic chemical vapor deposition method (MOCVD). The surface morphology and crystalline quality of these materials can be improved by a suitable choice of source compounds and by matching the lattice parameters of the epitaxial layer to the substrate [2, 7].

Electronic properties of some ternary semiconductor alloys have been computed in order to provide more information and knowledge about future device concepts and applications. Different theoretical methods have been used for the calculation of the properties of these alloys. The full potential linear augmented plane wave method (FP-LAPW) within the density functional theory (DFT) has been used to study the structural, electronic, thermodynamic and thermal properties of ZnSSe ternary alloys [8]. Ab initio pseudopotential calculations have been performed to study the structural properties of compounds based on elements such as Mg and Zn and the stability of MgSe–ZnSe ordered superlattices [9]. A study of the structural, electronic and optical properties of (BeTe/ZnSe) superlattices has been performed using the full potential linear muffin-tin orbital method (FP-LMTO) [10]. This method has also been used in order to investigate optoelectronic nature of MgCdSe alloys [11]. The electronic and optical properties of ZnS, ZnSe, CdS, CdSe and their alloy ZnCdSSe have been investigated using the empirical pseudopotential method (EPM) [12]. Also, with this method, the form factors and band structures for CdSe, CdS

*E-mail: k_benchikh2002@yahoo.fr

and ZnS have been determined [13]. Based on the pseudopotential scheme, the electronic properties of zinc-blende ZnMgSe alloys have been predicted [14]. Within the same empirical pseudopotential model, the electronic band structures of quaternary alloys CdZnSSe [15] and ZnMgSSe [16] have been calculated to study the structural, electronic and optical properties of these materials.

The empirical pseudopotential method (EPM) has been proven to be one of the most reliable methods for calculation of the band structures of semiconductors. In the EPM, the actual atomic potential is replaced by a pseudopotential and a group of atomic form factors are adjusted so that the calculations produced the energy bands as accurately as possible in the whole composition range in accordance with the existing experimental data.

The aim of this work is the study of electronic and optical properties of ternary alloys $Zn_xCd_{1-x}S$, $Zn_xCd_{1-x}Se$, ZnS_xSe_{1-x} and $Mg_xZn_{1-x}Se$ using the EPM method within the virtual crystal approximation (VCA) in order to complete the existing experimental and theoretical works on these alloys.

2. Computational method

In the EPM the empirical pseudopotential parameters (EPP) are considered as a superposition of pseudo-atomic potentials in the form:

$$V(r) = V_L(r) + V_{NL}(r) \quad (1)$$

where V_L and V_{NL} are local and non-local parts, respectively. In these calculations the non-local parts are not taken into account. We consider the Fourier components of $V_L(r)$ as the local EPPs. The used pseudopotential Hamiltonian is described by the following expression:

$$H = -\frac{\eta}{2m}\nabla^2 + V_L(r) \quad (2)$$

where $V_L(r)$ is the pseudopotential which can be expanded in the reciprocal lattice vectors G . For a binary compound the expansion is written in two elements, which are symmetrical and asymmetrical

with respect to an interchange of two atoms about their mid-point [9]:

$$V_L(r) = \sum_G [S^S(G)V^S(G) + iS^a(G)V^a(G)] \exp(iGr) \quad (3)$$

where $S(G)$ and $V(G)$ represent the structure and form factors, respectively.

The EPPs are determined by the nonlinear method of the least-squares where all parameters are simultaneously calculated under a defined criterion of minimizing the RMS deviation. The normal conditions are used for the experimental electronic band structure data. The nonlinear least-squares method requires that the RMS variation of the calculated level spacing (LSs) from the experimental ones, defined by:

$$\delta = \left(\frac{\sum_{(i,j)}^m (\Delta E^{(i,j)})^2}{m - N} \right)^{\frac{1}{2}} \quad (4)$$

was a minimum where:

$$\Delta E^{(i,j)} = E_{\text{exp}}^{(i,j)} - E_{\text{calc}}^{(i,j)}$$

Here, $E_{\text{exp}}^{(i,j)}$ and $E_{\text{calc}}^{(i,j)}$ are the observed and calculated LSs concerning the i -th state at the wave vector $k = k_i$ and the j -th at $k = k_j$, respectively, in the m cosen pairs (i,j) , while N is the number of EPPs. The energies obtained by solving the EPP secular equation are nonlinear functions of EPPs. The parameters starting values are improved step by step by iteration until δ is minimized. Let us denote the parameters by P_u ($u = 1, 2, \dots, N$) and write $P_u(n+1) = P_u(n) + \Delta P_u$, where $P_u(n)$ defines the value at the n -th iteration. The corrections ΔP_u are calculated at once by solving a system of linear equations:

$$\begin{aligned} \sum_{u=1}^N \left[\sum_{(i,j)}^m (Q_u^i - Q_u^j)(Q_{u'}^i - Q_{u'}^j) \right] \Delta P_u \\ = \sum_{(i,j)}^m \left[E_{\text{exp}}^{(i,j)} - E_{\text{calc}}^{(i,j)}(n) \right] (Q_{u'}^i - Q_{u'}^j) \\ u' = (1, 2, \dots, N) \end{aligned} \quad (5)$$

where $E_{\text{calc}}^{(i,j)}(n)$ is the value at the n -th iteration. Q_u is given by:

$$Q_u^j = \sum_{q,q'} [C_q^i(k_i)]^* \left(\frac{\partial H(k_i)}{\partial P_u} \right)_{q,q'} C_{q'}^j(k_i) \quad (6)$$

Here, $H(k_i)$ is the pseudohamiltonian matrix at $k = k_i$ in the plane wave representation and the i -th pseudowavefunction at $k = k_i$ is expanded as:

$$\psi_{k_i}^i(r) = \sum_q C_q^i(k_i) \exp[i(k_i + k_q)r] \quad (7)$$

where k_q is the reciprocal lattice vector. In equation 5 we can see that all of the parameters are computed automatically in an interdependent way. The lattice constant parameter of the ternary alloy $A_{1-x}B_xC$ is calculated via the Vegard's rule as:

$$a(x) = (1-x)a_{BC} + xa_{AC} \quad (8)$$

where a_{AC} and a_{BC} are the lattice constants of the parent binaries AC and BC, respectively. The alloy potential is calculated using the VCA, with the compositional disorder incorporated as an effective periodic potential:

$$V_{alloy}(r) = (1-x)V_{BC}(r) + xV_{AC}(r) - p[x(1-x)]^{1/2}[V_{AC}(r) - V_{BC}(r)] \quad (9)$$

where p is a parameter to be adjusted. We have used this potential for our alloy system over various compositions by changing p until an agreement with experiments was obtained.

3. Results and discussion

3.1. Electronic properties

In order to derive an accurate alloy band structure, we must begin from a realistic band structure of the ternaries under study. The adjusted pseudopotential form factors for binary parent compounds ZnS, ZnSe, CdS, CdSe and MgSe used in our calculation are listed in Table 1. In addition, the calculated and experimental energy gaps for the mentioned binary compounds are collected in Table 2 and show a reasonable agreement.

For MgSe we have adjusted the form factors reported in the literature [14] and taken the experimental energy values given in the literature [16]. The reason of this choice is the lack of experimental data in the literature. The energy band structures computed within EPM for the following ternary alloys $Zn_xCd_{1-x}S$, $Zn_xCd_{1-x}Se$, ZnS_xSe_{1-x} and $Mg_xZn_{1-x}Se$ are, respectively, shown in Fig. 1.

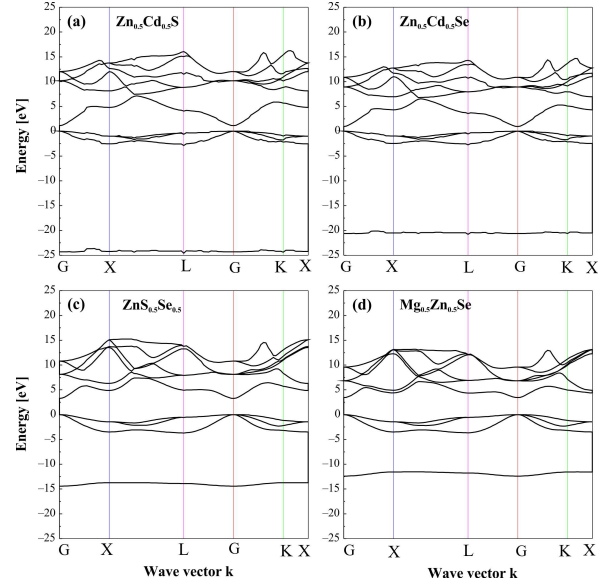


Fig. 1. Electronic band structure in zinc-blende (zb) phase for: (a) $Zn_{0.5}Cd_{0.5}S$, (b) $Zn_{0.5}Cd_{0.5}Se$, (c) $ZnS_{0.5}Se_{0.5}$, (d) $Mg_{0.5}Zn_{0.5}Se$.

In the present work the concentration $x = 0.5$ is chosen for all ternary alloys. The reference energy level is the top of the valence band assumed as zero energy and situated at the Γ symmetry direction of the first Brillouin zone. The curves in Fig. 1 exhibit a direct gap for the studied ternary alloys $Zn_xCd_{1-x}S$, $Zn_xCd_{1-x}Se$, ZnS_xSe_{1-x} and $Mg_xZn_{1-x}Se$ since the binaries ZnS, ZnSe, CdS, CdSe and MgSe are both direct gap compounds. We have found for the different ternary alloys the following energy gap values of 1.14 eV, 1.20 eV, 3.27 eV and 3.39 eV for $Zn_{0.5}Cd_{0.5}S$, $Zn_{0.5}Cd_{0.5}Se$, $ZnS_{0.5}Se_{0.5}$ and $Mg_{0.5}Zn_{0.5}Se$, respectively. Our results have been compared with the available experimental and theoretical data and have shown a good agreement [2].

The variation of the energy gaps ($E_{\Gamma\Gamma}$, $E_{\Gamma X}$, $E_{\Gamma L}$) versus the concentration x calculated within VCA only ($p = 0$) for the ternary alloys $Zn_xCd_{1-x}S$, $Zn_xCd_{1-x}Se$, ZnS_xSe_{1-x} and $Mg_xZn_{1-x}Se$ is presented in Fig. 2 to Fig. 5, respectively.

Referring to Fig. 2, Fig. 3 and Fig. 4, we observe that the ternary alloys $Zn_xCd_{1-x}S$, $Zn_xCd_{1-x}Se$ and ZnS_xSe_{1-x} have a direct band gap for all concentrations x ($0 \leq x \leq 1$).

Table 1. Adjusted form factors (in Ry) for the studied binaries.

| Material | V_S (3) | V_S (8) | V_S (11) | V_A (3) | V_A (4) | V_A (11) |
|----------|-----------|-----------|------------|-----------|-----------|------------|
| ZnS | -0.273609 | 0.041552 | 0.057521 | 0.207435 | 0.14000 | 0.04000 |
| CdS | -0.381411 | 0.068308 | -0.238828 | 0.311320 | 0.13000 | 0.223786 |
| ZnSe | -0.283115 | 0.056426 | 0.033312 | 0.178871 | 0.12300 | 0.053152 |
| CdSe | -0.293661 | 0.017887 | -0.156928 | 0.260615 | 0.12000 | 0.152888 |
| MgSe | -0.241454 | 0.026 | 0.05 | 0.15 | 0.089 | -0.03 |

Table 2. Calculated and experimental energy gaps for the binary compounds.

| Material | a [a.u.] | $E_{\Gamma\Gamma}$ [eV] | | $E_{\Gamma X}$ [eV] | | $E_{\Gamma L}$ [eV] | |
|----------|---------------------|-------------------------|-------------------|---------------------|-------------------|---------------------|-------------------|
| | | Calc. | Exp. | Calc. | Exp. | Calc. | Exp. |
| ZnS | 10.224 ^d | 3.51 ^a | 3.70 ^b | 5.23 ^a | 5.20 ^b | 5.28 ^a | 5.30 ^b |
| CdS | 11.021 ^d | 2.69 ^a | 2.50 ^b | 6.00 ^a | 6.00 ^b | 5.67 ^a | 5.60 ^b |
| ZnSe | 10.711 ^d | 2.68 ^a | 2.80 ^b | 4.49 ^a | 4.50 ^b | 4.47 ^a | 4.50 ^b |
| CdSe | 11.484 ^d | 2.01 ^a | 1.90 ^b | 5.41 ^a | 5.40 ^b | 4.74 ^a | 4.70 ^b |
| MgSe | 11.130 ^d | 4.21 ^a | 4.21 ^c | 4.13 ^a | 4.05 ^c | 4.19 ^a | 4.19 ^c |

^athis work, ^b[12], ^c[16], ^d[2]

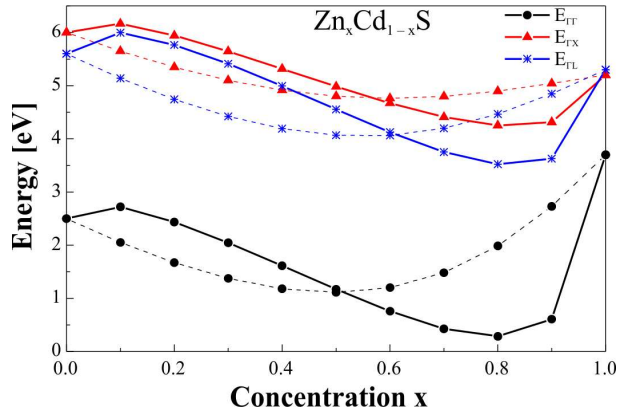


Fig. 2. Variation of energy gap with concentration for $Zn_xCd_{1-x}S$ in zb phase, obtained with VCA (dashed lines) and improved VCA (solid lines).

For ternary alloy ZnS_xSe_{1-x} the variation of the gaps increases with the x concentration. In the case of ternary alloys $Zn_xCd_{1-x}S$ and $Zn_xCd_{1-x}Se$, the variation of the gaps decreases with the x concentration for ($0 \leq x \leq 0.5$) and increases for ($0.5 < x \leq 1.0$) showing a bowing. For ternary alloy $Mg_xZn_{1-x}Se$, Fig. 5 shows a crossover from the direct gap to the indirect one. The energy gap

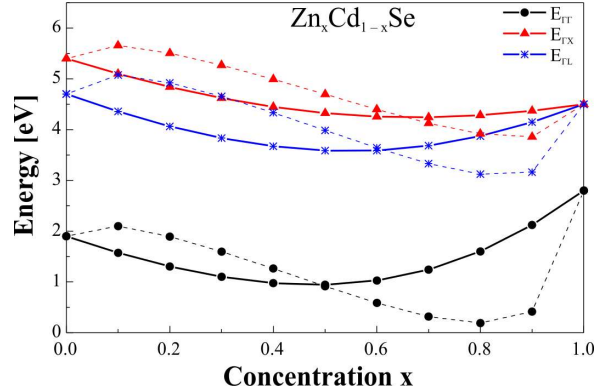


Fig. 3. Variation of energy gap with concentration for $Zn_xCd_{1-x}Se$ in zb phase, obtained with VCA (dashed lines) and improved VCA (solid lines).

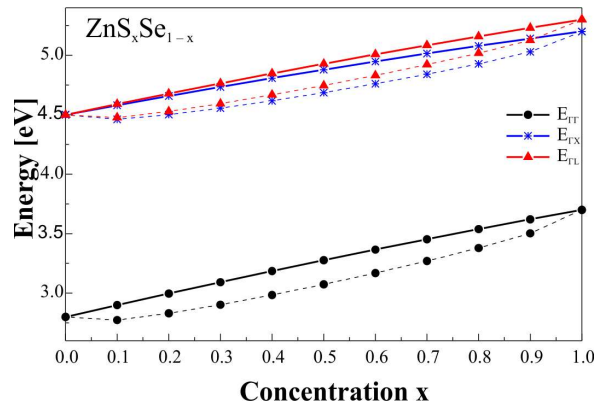


Fig. 4. Variation of energy gap with concentration for ZnS_xSe_{1-x} in zb phase, obtained with VCA (dashed lines) and improved VCA (solid lines).

of this crossover is 4.14 eV which corresponds to the concentration $x = 0.95$.

A quadratic fit of the obtained curves within VCA ($p = 0$), yields the following polynomial expressions of the three energy gaps $E_{\Gamma\Gamma}$, $E_{\Gamma X}$, $E_{\Gamma L}$ for the ternary alloys of interest:

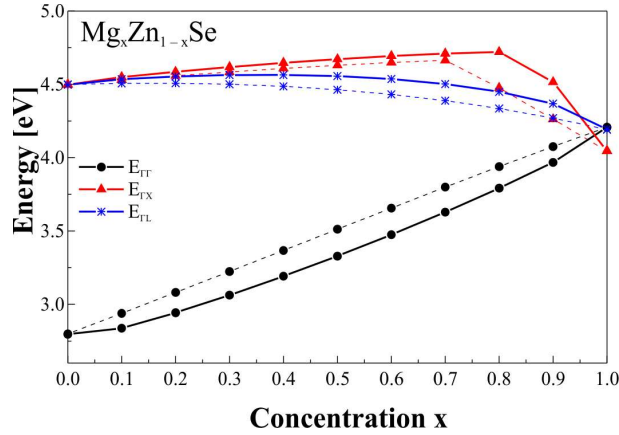


Fig. 5. Variation of the energy gap with concentration for $Mg_xZn_{1-x}Se$ in zb phase, obtained with VCA (dashed lines) and improved VCA (solid lines).

$$Zn_xCd_{1-x}S \Rightarrow \quad (10)$$

$$\begin{cases} E_{\Gamma\Gamma} = 2.695 - 7.147x + 7.964x^2 \\ E_{\Gamma X} = 6.007 - 3.969x + 3.197x^2 \\ E_{\Gamma L} = 5.671 - 5.928x + 5.539x^2 \end{cases} \text{VCA (p = 0)}$$

$$Zn_xCd_{1-x}Se \Rightarrow \quad (11)$$

$$\begin{cases} E_{\Gamma\Gamma} = 2.016 - 4.957x + 5.628x^2 \\ E_{\Gamma X} = 5.414 - 3.415x + 2.500x^2 \\ E_{\Gamma L} = 4.745 - 4.326x + 4.056x^2 \end{cases} \text{VCA (p = 0)}$$

$$ZnS_xSe_{1-x} \Rightarrow \quad (12)$$

$$\begin{cases} E_{\Gamma\Gamma} = 2.799 + 1.010x - 0.107x^2 \\ E_{\Gamma X} = 4.499 + 0.816x - 0.115x^2 \\ E_{\Gamma L} = 4.498 - 0.917x - 0.115x^2 \end{cases} \text{VCA (p = 0)}$$

$$Mg_xZn_{1-x}Se \Rightarrow \quad (13)$$

$$\begin{cases} E_{\Gamma\Gamma} = 2.793 + 1.456x - 0.035x^2 \\ E_{\Gamma X} = 4.403 + 1.286x - 1.556x^2 \\ E_{\Gamma L} = 4.493 + 0.175x - 0.470x^2 \end{cases} \text{VCA (p = 0)}$$

The results for the energy gap curves presented in Fig. 2 to Fig. 5 show clearly that without the disorder potential ($p = 0$) the EPP approach within the VCA does not produce the true band gap bowing.

The observed bowing parameters C_{exp} can be estimated by the sum of two terms C_i and C_e where C_i is the intrinsic bowing parameter due to order effects which exist already in a fictitiously periodic alloy, and C_e is the extrinsic bowing parameter due to disorder effects:

$$C_{exp} = C_i + C_e \quad (14)$$

Our treatment is extended through the use of the improved VCA which takes into account the effects of the compositional disorder by tuning the p parameter. The computed curves within the improved VCA are shown in Fig. 2 to Fig. 5 for ternary alloys $Zn_xCd_{1-x}S$, $Zn_xCd_{1-x}Se$, ZnS_xSe_{1-x} and $Mg_xZn_{1-x}Se$, respectively.

After a least-squares fit the resulted curves show sublinearity, yielding the quadratic terms presented as the bowing parameters in Table 3 and the following relations of the energy gaps:

$$Zn_xCd_{1-x}S \Rightarrow \quad (15)$$

$$\begin{cases} E_{\Gamma\Gamma} = 2.879 - 3.698x + 0.848x^2 \\ E_{\Gamma X} = 6.257 - 2.464x + 0.077x^2 \\ E_{\Gamma L} = 5.996 - 2.342x + 0.725x^2 \end{cases} \text{improved VCA}$$

$$Zn_xCd_{1-x}Se \Rightarrow \quad (16)$$

$$\begin{cases} E_{\Gamma\Gamma} = 2.199 - 2.648x + 0.384x^2 \\ E_{\Gamma X} = 5.638 - 1.252x - 1.023x^2 \\ E_{\Gamma L} = 5.023 - 1.386x - 1.075x^2 \end{cases} \text{improved VCA}$$

$$ZnS_xSe_{1-x} \Rightarrow \quad (17)$$

$$\begin{cases} E_{\Gamma\Gamma} = 2.767 + 0.292x + 0.595x^2 \\ E_{\Gamma X} = 4.469 + 0.137x + 0.548x^2 \\ E_{\Gamma L} = 4.470 + 0.274x + 0.516x^2 \end{cases} \text{improved VCA}$$

$$Mg_xZn_{1-x}Se \Rightarrow \quad (18)$$

$$\begin{cases} E_{\Gamma\Gamma} = 2.773 + 0.794x + 0.600x^2 \\ E_{\Gamma X} = 4.473 + 0.781x - 0.718x^2 \\ E_{\Gamma L} = 4.493 + 0.443x - 0.634x^2 \end{cases} \text{improved VCA}$$

The compositional disorder effect can be explained from equation 10 to equation 13, and equation 15 to equation 18. With improved VCA in

Table 3. Bowing parameters for the energy gaps $E_{\Gamma\Gamma}$, $E_{\Gamma X}$, $E_{\Gamma L}$ within improved VCA.

| | p | $E_{\Gamma\Gamma}$ [eV] | $E_{\Gamma X}$ [eV] | $E_{\Gamma L}$ [eV] |
|------------------|---------------------------------------|-------------------------------------------------------------|---------------------|---------------------|
| $Zn_xCd_{1-x}S$ | 1.05 ^a | 0.848 ^a , 0.827 ^b | 0.077 ^a | 0.725 ^a |
| $Zn_xCd_{1-x}Se$ | 1.205 ^a | 0.384 ^a , 0.387 ^b | -1.023 ^a | -1.075 ^a |
| ZnS_xSe_{1-x} | 0.28 ^a | 0.595 ^a , 0.580 ^b , 0.46 ^d | 0.548 ^a | 0.516 ^a |
| $Mg_xZn_{1-x}Se$ | 0.34 ^a , 0.72 ^c | 0.600 ^a , 0.600 ^b , 0.4 ^c | -0.718 ^a | -0.634 ^a |

^athis work, ^b[2], ^c[14], ^d[17]

the case of $E_{\Gamma\Gamma}$, our results compared to those obtained with VCA, show that the bowing parameters decrease for $Zn_xCd_{1-x}S$ and $Zn_xCd_{1-x}Se$ on one hand and increase for ZnS_xSe_{1-x} and $Mg_xZn_{1-x}Se$ on the other hand. Thus, the improved VCA reproduces the disorder effect. From Table 3 our results are seen to be in good agreement with the available experimental data.

3.2. Optical properties

The refractive index (n) is a very important parameter associated to the atomic interactions. Thus, many attempts have been performed in order to obtain simple relationships between the refractive index (n) and the energy gap ($E_{\Gamma\Gamma}$) [18, 19]. In this work, we present the calculated variation of n with alloy concentration using the following three models: Moss model [20], Ravindra model [21], and Herve and Vandamme model [22].

The Moss model is based on the following expression:

$$n^4 E_g = k \quad (19)$$

where $k = 108$ and E_g is the energy band gap $E_{\Gamma\Gamma}$.

Ravindra presented a linear form of n as a function of E_g :

$$n = \alpha + \beta E_g \quad (20)$$

with $\alpha = 4.084 \text{ eV}^{-1}$ and $\beta = -0.62 \text{ eV}^{-1}$.

An empirical function of n has been proposed by Hervé and Vandamme as follows:

$$n = \sqrt[2]{1 + \left(\frac{A}{E_g + B}\right)^2} \quad (21)$$

with $A = 13.6 \text{ eV}$ and $B = 3.4 \text{ eV}$.

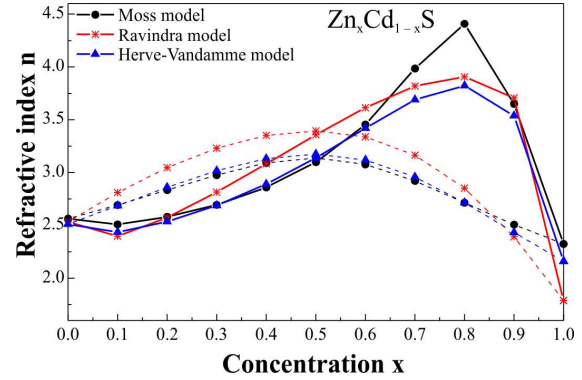


Fig. 6. Variation of refractive index as a function of concentration x for $Zn_xCd_{1-x}S$, obtained with VCA (dashed lines) and improved VCA (solid lines).

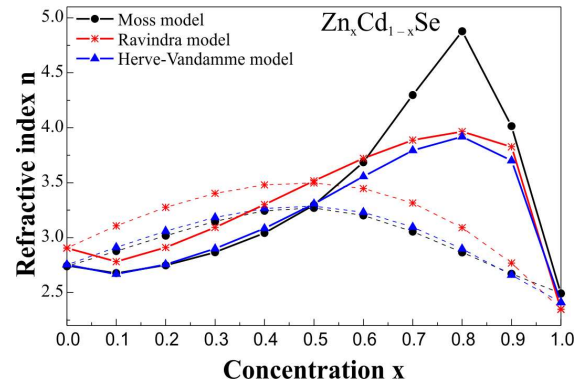


Fig. 7. Variation of refractive index as a function of concentration x for $Zn_xCd_{1-x}Se$, obtained with VCA (dashed lines) and improved VCA (solid lines).

In the present work, we have calculated the variation of the refractive index n with alloy concentration x as well with VCA ($p = 0$) then with improved VCA, by using these three models. The resulting curves are presented in Fig. 6 to Fig. 9, respectively.

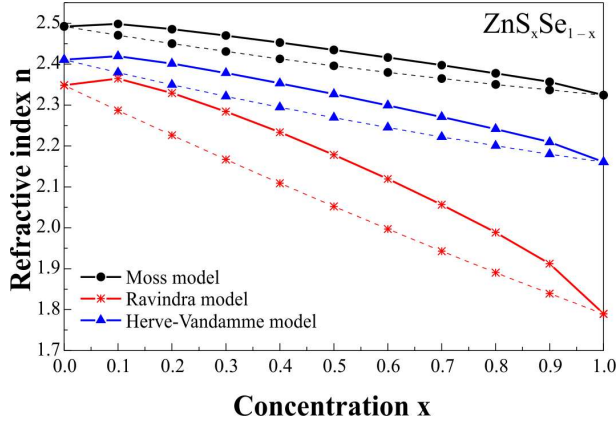


Fig. 8. Variation of refractive index as a function of concentration x for ZnS_xSe_{1-x} , obtained with VCA (dashed lines) and improved VCA (solid lines).

The variation of n was determined by polynomial fitting. In our work the best fit yields the following expressions for the ternary alloys $Zn_xCd_{1-x}S$, $Zn_xCd_{1-x}Se$, ZnS_xSe_{1-x} and $Mg_xZn_{1-x}Se$, respectively:

$$Zn_xCd_{1-x}S \Rightarrow \quad (22)$$

$$\left\{ \begin{array}{l} n(x) = 2.126 + 3.960x - 2.867x^2 \\ \text{Moss model} \\ n(x) = 2.012 + 5.237x - 4.505x^2 \\ \text{Ravindra model} \\ n(x) = 2.104 + 3.954x - 3.132x^2 \\ \text{Hervé-Vandamme model} \end{array} \right.$$

$$Zn_xCd_{1-x}Se \Rightarrow \quad (23)$$

$$\left\{ \begin{array}{l} n(x) = 2.261 + 4.232x - 2.961x^2 \\ \text{Moss model} \\ n(x) = 2.496 + 3.938x - 3.342x^2 \\ \text{Ravindra model} \\ n(x) = 2.337 + 3.536x - 2.794x^2 \\ \text{Hervé-Vandamme model} \end{array} \right.$$

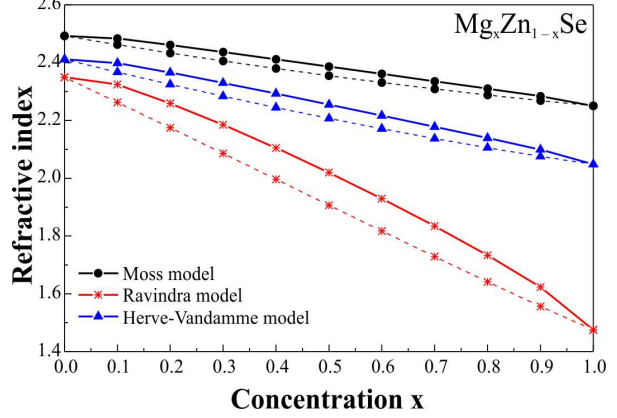


Fig. 9. Variation of refractive index as a function of concentration x for $Mg_xZn_{1-x}Se$, obtained with VCA (dashed lines) and improved VCA (solid lines).

$$ZnS_xSe_{1-x} \Rightarrow \quad (24)$$

$$\left\{ \begin{array}{l} n(x) = 2.499 - 0.073x - 0.099x^2 \\ \text{Moss model} \\ n(x) = 2.364 - 0.144x - 0.418x^2 \\ \text{Ravindra model} \\ n(x) = 2.421 - 0.103x - 0.155x^2 \\ \text{Hervé-Vandamme model} \end{array} \right.$$

$$Mg_xZn_{1-x}Se \Rightarrow \quad (25)$$

$$\left\{ \begin{array}{l} n(x) = 2.498 - 0.192x - 0.054x^2 \\ \text{Moss model} \\ n(x) = 2.361 - 0.461x - 0.414x^2 \\ \text{Ravindra model} \\ n(x) = 2.419 - 0.277x - 0.093x^2 \\ \text{Hervé-Vand. model} \end{array} \right.$$

The improved VCA reproduces very well the refractive index which presents a nonlinear variation on the x concentration as illustrated in the plotted graphs in Fig. 6 to Fig. 9. Also, the behavior of n is opposite to the one of $E_{\Gamma\Gamma}$ for the three models and the four ternary alloys. This behavior has been observed in the majority of II-VI compounds. The calculated refractive index values of the endpoint compounds are listed in Table 4. A good agreement is observed with results of other authors for ZnS and ZnSe when using the three models.

Table 4. Refractive indices for used binaries.

| | ZnS | CdS | ZnSe | CdSe | MgSe |
|--------------------|---------------------------------------|-------------------|-----------------------------------------------------------|-------------------|-------------------|
| n (Moss) | 2.32 ^a , 2.32 ^b | 2.12 ^a | 2.49 ^a , 2.51 ^b | 2.26 ^a | 2.25 ^a |
| n (Ravindra) | 1.80 ^a , 1.79 ^b | 2.01 ^a | 2.36 ^a , 2.42 ^b , 2.27 ^c | 2.49 ^a | 1.48 ^a |
| n (Hervé-Vandamme) | 2.16 ^a , 2.15 ^b | 2.10 ^a | 2.42 ^a , 2.48 ^b , 2.38 ^c | 2.37 ^a | 2.05 ^a |

^athis work, ^b[17], ^c[12]

4. Conclusions

The empirical pseudopotential method within VCA and improved VCA has been used to calculate the electronic and optical properties of ternary alloys $Zn_xCd_{1-x}S$, $Zn_xCd_{1-x}Se$, $Zn_xS_xSe_{1-x}$ and $Mg_xZn_{1-x}Se$. In the present work it is shown that the calculated band structures for all the alloys are characterized by a direct band gap except for the $Mg_xZn_{1-x}Se$ alloy which presents a crossover from the direct gap to the indirect one. An empirical bowing parameter has been introduced into the VCA expression. It is observed that the band gap bowing can be obtained with fairly good agreement with experiment. On the other hand, the refractive index of the considered ternary alloys has been calculated using three different models. The results of the analysis show the nonlinear dependence of the refractive index with concentration. In general, an overall agreement between the calculated and measured results has been obtained.

References

- [1] FUJITA S., *Jpn. J. Appl. Phys.*, 54 (2015), 030101.
- [2] ADACHI S., *Properties of semiconductor alloys: Group IV, III-V and II-VI Semiconductors*, John Wiley & Sons, Ltd., 2009.
- [3] VETCHEN VAN J., BERGSTRESSER T., *Phys. Rev. B*, 1 (1970), 3351.
- [4] HILL R., *J. Phys. C Solid State Phys.*, 7 (1974), 521.
- [5] JAROS M., *Rep. Prog. Phys.*, 48 (1985), 1091.
- [6] AYMERICH F., *Phys. Rev. B*, 26 (1982), 1968.
- [7] KUKIMOTO H., *Mater. Res. Soc. Sym. Proc.*, 161 (1990).
- [8] BENDAIF S., BOUMAZA A., NEMIRI O., BOUBENDIRA K., MERADJI H., GHEMID S., EL HAJ HASSAN F., *B. Mater. Sci.*, 38 (2015), 365.
- [9] LEE S.G., CHANG K., *Phys. Rev. B*, 52 (1995), 1918.
- [10] CAID M., RACHED H., RACHED D., KHENATA R., BIN OMRAN S., VASHNEY D., ABIDRI B., BENKHETTOU N., CHAHED A., BENHELLAL O., *Mater. Sci.-Poland*, 34 (2016), 115.
- [11] BENSALD D., AMERI M., EL HANANI M., AZAZ Y., BENDOUA M., AL-DOURI Y., AMERI I., *Mater. Sci.-Poland*, 32 (2014), 719.
- [12] BOUKORTT A., ABBAR B., ABID H., SEHIL M., BENSALD Z., SOUDINI B., *Mater. Chem. Phys.*, 82 (2003), 911.
- [13] BERGSTRESSER T., COHEN M.L., *Phys. Rev.*, 164 (1967), 1069.
- [14] CHARIFI Z., BAAZIZ Z., BOUARISSA N., *Mater. Chem. Phys.*, 84 (2004), 273.
- [15] KWON S.J., JEONG H.M., JUNG K., KO D.H., KO H., HAN I.K., KIM G.T., PARK J.G., *ACS Nano*, 9 (2015), 5486.
- [16] TEO K., FENG Y., LI M., CHONG T., XIA J., *Semi-cond. Sci. Tech.*, 9 (1994) 349.
- [17] BENKABOU K., AOUMEUR F., ABID H., AMRANE N., *Physica B*, 337 (2003), 147.
- [18] RUOFF A., *Mater. Res. Soc. Symp. Proc.*, 22 (1984), 287.
- [19] REDDY R., ANJANEYULU S., SARMA C., *J. Phys. Chem. Solids*, 54 (1993), 635.
- [20] MOSS T., *Proc. Phys. Soc. B*, 63 (1950), 167.
- [21] RAVINDRA N., SRIVASTAVA V., *Infrared Phys. Techn.*, 19 (1979), 603.
- [22] HERVÉ P., VANDAMME L.K.J., *Infrared Phys. Techn.*, 35 (1994), 609.

Received 2016-05-01

Accepted 2016-11-23